二次精錬プロセスへの不焼成マグネシアれんがの応用

Application of unburned magnesia bricks for steel secondary refining processes

冨田雄也[*]，阿南貴大[**]，後藤　潔[***]，森川勝美[****]
Yuya TOMITA[*], Takahiro ANAN[**], Kiyoshi GOTO[***] and Katsumi MORIKAWA[****]

要　旨

二次精錬プロセス用の耐火物として，マグクロれんがやマグネシアカーボンれんがが広く使用されている。しかしマグクロれんがは環境に有害な六価クロムの生成，マグネシアカーボンれんがには，熱ロスの課題がある。そこで，将来の環境問題の観点から，クロムも黒鉛も含まない二次精錬用の不焼成マグネシアれんがを開発した。開発したれんがの特筆すべき点は，FeO に対する耐食性が従来のマグクロれんが，マグネシアカーボンれんがと比較して優れていることである。このように，新たに開発した環境面にも優しい不焼成のマグネシアれんがは，二酸化炭素排出量の削減だけではなく，クロムの除去にも貢献できる。

Abstract

In the steel refining processes, magnesia carbon or magnesia chrome bricks have been widely used conventionally as refractories for holding molten steel to be refined due mainly to satisfy the material requirement for high corrosion resistant. However, magnesia carbon bricks and magnesia chrome bricks have heat loss and hexavalent chromium formation problems, respectively. A novel unburned magnesia brick have been developed for use in the steel secondary refining process that contains neither graphite nor chromium, in light of future environmental issues. As a notifying point of the developed brick, the high temperature corrosion resistance against iron oxide, FeO was superior to the conventional magnesia-carbon and -chromite bricks. Thus, newly developed environmentally friendly unburned magnesia brick will be contributing not only in the reduction of CO_2 and carbon neutrality but also in the elimination of chromium.

1　緒言

マグクロれんがとマグネシアカーボンれんがは，二次精錬炉で広く使用されている。

マグクロれんがは溶鋼中のアルカリ成分と反応し，有害な 6 価クロムを生成しやすいという問題があり，この対策としてクロムフリー材質の開発が検討されている[1-4)]。

また，二酸化炭素排出量の削減に対する取り組みが, 産業界でさらに求められることが考えられる。特に，マグクロれんがは 1700 ℃以上で焼成されており，焼成時に大量の二酸化炭素を排出している。

1 Introduction

Magnesia carbon (MgO-C) bricks and magnesia chrome ($MgO-Cr_2O_3$) bricks with high corrosion resistance are used widely in the secondary refining processes of steel.

Magnesia chrome bricks easily react with alkaline components in the molten steel and produce harmful hexavalent chromium compound The development of chromium-free material is examined as a countermeasure against the problem [1- 4)].

In future, the challenge for CO_2 reduction and carbon neutrality will be required more keenly for industrial world. $MgO-Cr_2O_3$ bricks are fired at temeratures higher than 1700 ℃, and a large amount

＊　技術研究所 製品プロセス研究センター アシスタントマネージャー　Assistant Manager, Product R&D Center, Technical Research Institute
＊＊　窯炉製造事業部 瀬戸内工場 マネージャー　Manager, Setouchi Plant, Furnace Refractories Division
＊＊＊　フェロー 技術研究所 所長　Fellow, General Manager, Technical Research Institute
＊＊＊＊　技術研究所　エグゼクティブアドバイザー　Executive adviser, Technical Research Institute

Ghoshらの報告[5, 6]では，200 ℃で熱処理された不焼成マグクロれんがが二次精錬炉で使用され，焼成マグクロれんがと同等の耐食性を示したことが報告されている。

一方で，マグネシアカーボンれんがは，黒鉛を含有しており熱伝導率の上昇による熱放散の増加や溶鋼中へのカーボンの溶出が懸念される。田中らの報告[7]では，転炉に低黒鉛質のマグネシアカーボンれんがを適用することで，熱ロスが 17 % 抑制され，れんがの耐用も向上したことが報告されている。

これらの状況を考慮し，二次精錬炉に適用可能な，クロムも黒鉛も含まない不焼成のマグネシアれんがを開発した。今回の報告では，開発したれんがの特性の評価と実際の炉で使用した時の熱ロス抑制の効果を調査した。

2　試験方法

2・1　供試試料

表 1 に示すように黒鉛を含まない不焼成のマグネシアれんがと黒鉛添加量が 1, 3, 5 mass% のマグネシアカーボンれんが（試料名：A ～ D）と，比較としてダイレクトボンドのマグクロれんがを評価した。A ～ D の試料は，酸化防止剤を適量添加し，その添加量は一定とした。これらを適量のフェノール樹脂とともに混練後，真空オイルプレスで 230 × 100 × 110 mm に成形し，250 ℃で 5 時間乾燥して試料を作製した。

of carbon dioxide is emitted during production. An unburned MgO-Cr_2O_3 brick tempered at 200 ℃ for the secondary refining was examined and reported to have corrosion resistance equivalent to that of fired MgO-Cr_2O_3 bricks [5, 6].

Since the MgO-C bricks contain flake graphite, there are concerns about heat dissipation into the atmosphere due to increased thermal conductivity and carbon leaching into the molten steel. It was reported that applying low graphite MgO-C bricks to the converters, the heat loss could be reduced by 17 % with improved durability of the brick [7].

Considering these situations, we also have examined to develop an unburned magnesia brick for the secondary refining without containing neither chromium nor graphite. In the present study, the characteristics of the developed bricks were investigated, together with the effect of heat loss control when used in an actual furnace.

2 Experimental Procedure

2・1 Test Materials

The unburned magnesia (MgO) bricks without containing graphite and MgO-C bricks with the graphite contents of 1, 3, and 5 % were named materials A to D, respectively. They were chosen as test materials together with material E of a direct bonded MgO-Cr_2O_3 brick for comparison, as shown in **Table 1**. Raw materials powders for the test materials A to D were mixed with both suitable amounts of phenol resin as binder, and some antioxidant agent, molded and formed to 230×100×110 mm shape bar using a vacuum hydraulic press, then dried at 250 ℃ for 5 h to prepare the test samples.

Table 1 Composition of test materials A~E

	Material (Category)	A	B	C	D	E
		MgO	MgO-C			MgO-Cr_2O_3
Composition / mass%	MgO	100	99	97	95	54
	Cr_2O_3	-	-	-	-	31
	Al_2O_3	-	-	-	-	7
	C(Graphite)	-	1	3	5	-

Table 2 Bulk density and porosity of materials A~ E

Material / Density/Porosity	A	B	C	D	E
	MgO	MgO-C			$MgO\text{-}Cr_2O_3$
Bulk density / × $10^3 kg・m^{-3}$	3.14 (3.15)	3.14 (3.16)	3.12 (3.15)	3.08 (3.10)	3.27
Apparent porosity / %	9.0 (5.4)	8.3 (4.3)	8.2 (3.5)	8.3 (3.0)	15.6

( ) : After drying

2・2　評価方法

2・2・1　かさ密度，気孔率

密度，気孔率は，JIS R 2205 に基づき測定した。尚，Ａ～Ｄの試料は，**表 2** に示すように乾燥後及び 1400 ℃で 3 時間還元焼成後の状態でそれぞれの試料において行った。比較として焼成後のマグクロれんがも評価した。

2・2・2　熱伝導率及び高熱 Fe-oxide 侵食試験

熱伝導率の測定は 1400 ℃で 3 時間還元焼成した試料において，800 ℃で熱流法を用いて行った。次に，高熱 Fe-oxide 侵食試験は，あらかじめ 1400 ℃で 3 時間還元焼成した試料を，1750 ℃まで昇温した後 30 分間保持して鋼製ランスから酸素を吹き込み，ランス先端での酸化発熱により発生した高温下において，生成した Fe-oxide によりれんがを侵食させる方法により行った [8)]。その装置及び方法の概略を**図 1** に示す。

2・2 Test Method

2・2・1 Density and Porosity

Bulk density and porosity were measured based on JIS R 2205. The measurements were carried out for each sample for materials A to D after drying and after firing at 1400 ℃ for 3 h under the reducing atmosphere as shown in **Table 2**. As a comparision the direct bonded magnesia chrome brick (E) after fired was also evaluated.

2・2・2 Thermal Property and Corrosion

The thermal conductivity was measured at 800 ℃ using the heat flow method in the specimen after the firing at 1400 ℃ for 3 h.

Figure 1 shows a schematic of the apparatus and method of high-temperature Fe-oxide corrosion test. The test was carried out by a method in which a specimen, which had been reduced and fired at 1400 ℃ for 3 h in advance, was heated to 1750 ℃ and held for 30 min, oxygen was blown from a steel lance, and the brick was corroded by the Fe-oxide formed with heat generated by oxidation reaction in th the lance tip under a high temperature [8)]. The degree of

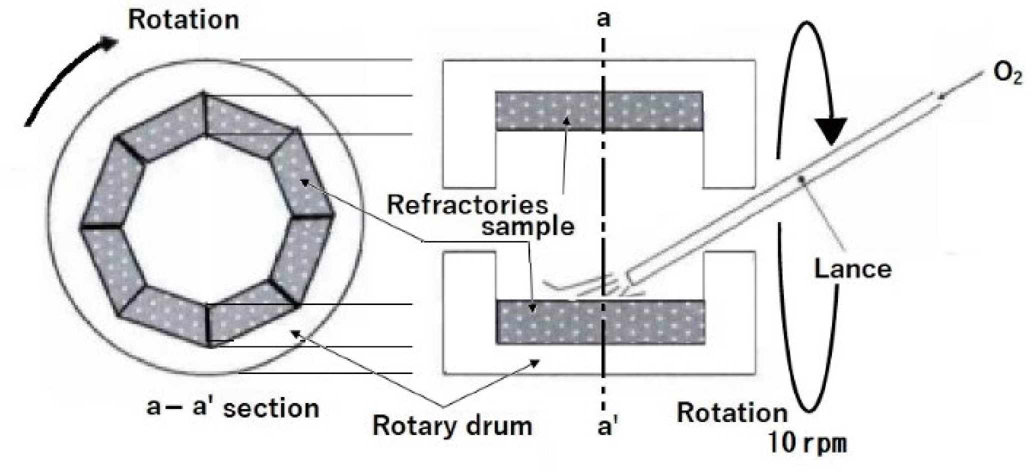

Fig. 1 Schematic image of high temperature Fe-oxide test.

耐食性の評価は，試験前後の試料の溶損量の測定と稼働面組織の微構造を観察した。溶損量はマグクロれんがの溶損量を 100 として溶損指数として評価した。微構造の観察は，SEM および EPMA を用いて観察した。

3　結果および考察

3・1　かさ密度，見かけ気孔率

表 2 に試料 A ～ D の乾燥後及び 1400 ℃で 3 時間還元焼成後，焼成後の試料 E の物性を示す。**図 2** に乾燥後，1400 ℃で 3 時間還元焼成後のかさ密度 (a)，見掛気孔率 (b) に及ぼす黒鉛の添加量の影響を示す。

まず，かさ密度は，乾燥後と焼成後の両方の場合で，1 mass% 以上の添加で，黒鉛添加量の増大とともに低下する傾向を示したが，0 mass%（黒鉛を含まない）の場合，最も高い 1 mass% 添加の場合よりも低い値であった。次に，気孔率は，乾燥後の場合は，黒鉛添加量の増大とともに単調に低下する傾向を示したが，焼成後では，黒鉛添加により低下するものの，1 mass% 以上の添加でほぼ一定値を示した。

corrosion was evaluated by measuring the amount of errosion in a cut surface of the specimen after the corrosion test and in addition to the microstructure observation in the cross section of the specimen at the vicinity of corroded surface after the high temperature Fe-oxide test.

Assessment of the corrosion behavior was performed by two methods; a direct measurement of the amount of corrosion and an analysis of microstructural observation of corroded surface. In the former assessment, measured amount of corrosion for each sample was converted to corrosion index to compare the amount relatively by setting the amount of corrosion for $MgO\text{-}Cr_2O_3$ to 100. Microstructural observation as an another assessment, was carried out in the specimen obtained from the cross section of the sample for each material at the vicinity of corroded surface using scanning electron microscope (SEM) including detail analysis using EPMA (Electron probe micro-analyzer).

3 Experimental Results and Discussion

3・1 Bulk Density and Apparent Porosity

Table 2 shows the physical properties of materials (A-D) after dried and after fired at 1400 ℃ for 3 h and material (E) after firing as a conpmarision. **Figure 2** shows the variations of bulk density (a), apparent porosity (b) with amount of graphite addition for both dried and fired states.

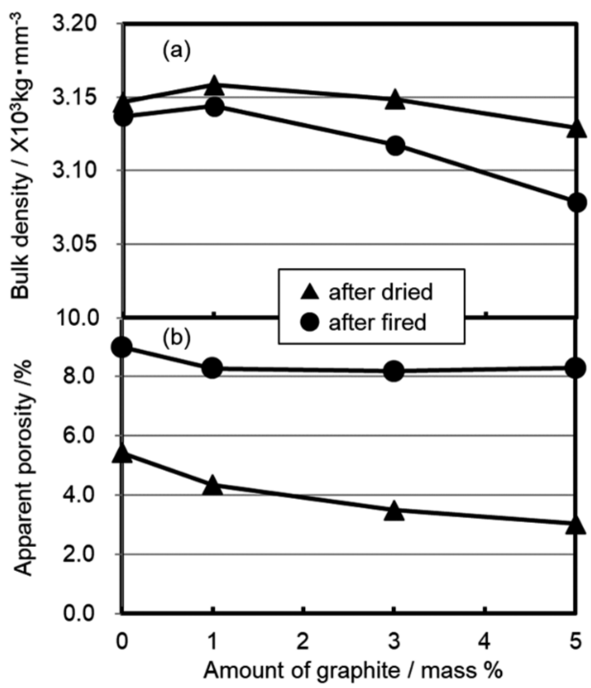

Fig. 2 Variations of bulk density (a) and apparent porosity (b) with amount of graphite addition for both dried and fired states.

3・2　熱伝導率及び高熱 Fe-oxide 侵食試験

図 3 (a) と **(b)** に，800 ℃における熱伝導率と高熱 Fe-oxide 試験の溶損指数の黒鉛の添加量の影響をそれぞれ示す。熱伝導率は，黒鉛の添加量が少ないほど低くなり，黒鉛を含まないれんがの熱伝導率は，黒鉛添加量 5 mass% の場合と比べると，約 50 %低下することが分かった。黒鉛を含まないれんがの熱伝導率は，ダイレクトボンドのマグクロれんがとほとんど同じ値となった。

マグクロれんがの溶損指数を 100 とすると，マグネシアカーボンれんがの溶損指数はマグクロれんがと比較するとかなり小さく，黒鉛の添加量が少ないほど耐食性が向上していることが分かる。

焼成後のマグネシアカーボンれんがの耐食性は，見掛気孔率が低いほど耐食性が向上することが報告されている [9]。**図 3 (b)** に示すように，黒鉛を含まないれんがは他のマグネシアカーボンれんがと比較して焼成後の見掛気孔率が高いにも関わらず，高熱 Fe-oxide 試験の耐食性は向上した。この原因を調査するために，高熱 Fe-oxide 試験の試験後の試料の稼働面組織を観察した。

First, the bulk density showed a tendency to increase with the graphite addition for the amount up to 1 % then, decrease with exceeding addition to 1 % for both dried and fired states. Next, the apparent porosity tended to decrease with increase in the graphite addition for after dried states, and showed almost constant value in the case of the addition exceeding 1 %, though it slightly decreased with the graphite addition for after fired states.

3・2 Thermal Conductivity and High Temperature Corrosion

The dependences of the graphite addition amount on the thermal conductivity at 800℃ and the corrosion index in the high temperature Fe-oxide test are shown in **Fig. 3 (a)** and **(b)**, respectively. Decreasing the graphite content, the thermal conductivity lowers to the minimal value with 0 % addition, resulting in the 50 % reduction from the value with 5 % graphite. The thermal conductivity value of the material without graphite is almost the same value of the direct bonded $MgO\text{-}Cr_2O_3$ brick.

Supposing the corrosion index of the magnesia chromite specimen as 100, the index of MgO-C bricks was much lower than that of the magnesia chromite brick and the index lowered with decreasing the graphite indicating the improvement in the corrosion resistance.

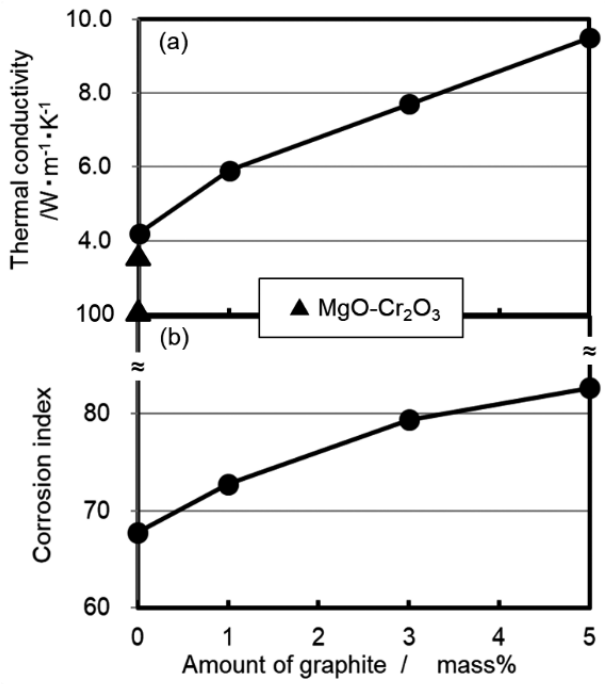

Fig. 3 Variation of thermal conductivity (a) and corrosion index obtained by the high temperature Fe-oxide test (b) with amount of graphite addition.

3・3　稼働面の微構造

図 4 に高熱 Fe-oxide 試験後の黒鉛添加量 5 mass% の試料 D(a)，黒鉛を含まない試料 A(b)，ダイレクトボンドのマグクロれんが E(c) の稼働面組織を示す。

黒鉛添加量 5 mass% の試料 D(a)，黒鉛を含まない試料 A(b) は，いずれの試料においても稼働面に MgO の連続層の形成が見られるものの，(a) では大きな空隙の介在により連続性に乏しく，連続層の下の試料内部には，MgO-C 反応によって生じたと思われる空隙が見られた。一方，(b) では，連続層内には大きな空隙は存在せず，強固な連続

The corrosion resistance of the MgO-C bricks after firing has been reported to be affected by the porosity in the manner in which the corrosion resistance became higher with lowering the porosity [9]. As shown in the **Fig. 3 (b)**, the corrosion resistance against Fe-oxide at high temperature was improved in the bricks without graphite, although the porosity after firing was higher than in the other bricks. To investigate the reason why this occurred, we have carefully observed the microstructure at the vicinity of corroded test surface of the specimen after high temperature Fe-oxide test.

3・3 Microstructure of Corroded Surface of Bricks

Figure 4 shows the microstructures at the

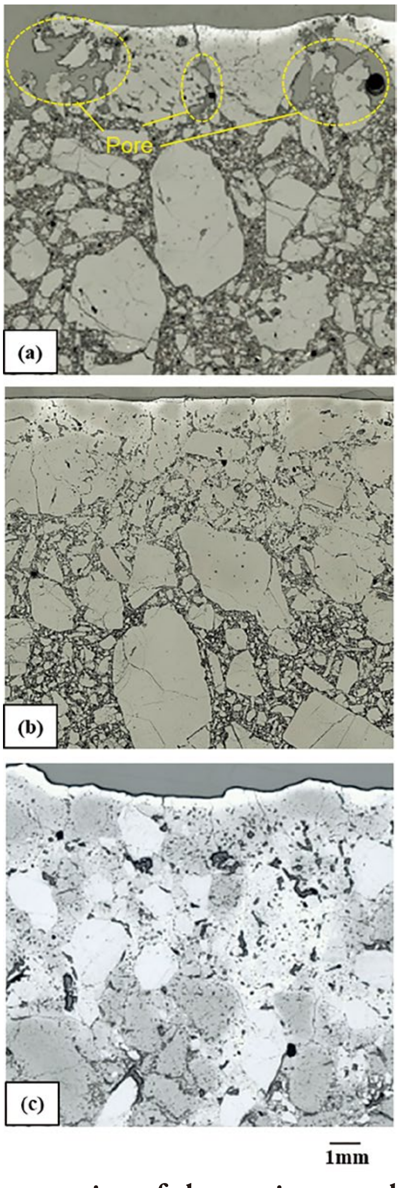

Fig. 4 Microstructure of the cross section of the specimen at the vicinity of surface after high temperature Fe-oxide corrosion test for materials A, D and E for (a), (b) and (c), respectively.

性が保たれ，連続層の下の試料内部における空隙の生成は，（a）と比較して大幅に抑制されていることが分かる。

以上のことから，黒鉛を含まない試料においては，高熱侵食試験後の稼働面近傍に形成されるMgO クリンカーが強固に連結し，れんが組織に空隙が生じ難く，この連続層が MgO-C 反応によるMg の逸散，Fe-oxide の侵入を抑制することによって，内部を保護するために優れた耐食性を示したものと考えられた。

最も耐食性が悪い結果であった (c) の場合，(b)のように大きな空隙は存在しないことが分かる。一方で試料E(c)は，試料A(b)と試料D(a)とは異なり，骨材の形状が不明瞭になっていることが分かる。

試料 A(b) と試料 E(c) の溶損の違いを調査するために，EPMA を用いて稼働面の微構造を観察した。**図 5** に高熱 Fe-oxide 試験後の試料 A(a) と試料 E(b) の稼働面組織を示す。鉄の元素分布に着目すると，試料 A(a) では稼働面近傍に鉄が残っているのに対して，試料 E(b) では鉄が組織の内部まで浸潤していることが分かる。このように，試料A(a) は，試料 E(b) よりも鉄の浸潤が抑制されたため優れた耐食性を示したことが考えられた。

3・4　熱放散抑制効果

表 1 に示した供試 4 材質を，それぞれ**図 6** に示す RH 真空脱ガス装置下部槽側面内層壁（ウェアれんがとして）で適用した場合を想定し，同図 (a)縦断面において破線で囲んだ部分を (b) のように，中心からウェアれんがの稼働面までの距離が 1000 mm，高さが 2500 mm の円筒へと簡略化したモデルとして定常熱伝導計算を行った。計算にあたっては，壁面の層構成とそれぞれの厚さおよび熱伝導率を**表 3 (1)** に示すような各数値を計算条件とした。なお，ここで，ウェアれんが 4 材質の熱伝導率は，**図 3 (a)** で示した測定値を用いた。

定常熱伝導を仮定し，下部槽最外層の鉄皮表面からの放熱量を算出するにあたり，稼働面側（内層）の温度を 1600 ℃とし，鉄皮表面は外気温度

vicinity of corroded test surface of the cross section after high temperature Fe-oxide test for materials with (a) 5 %, (b) 0 % graphite and (c) the direct bonded $MgO-Cr_2O_3$ brick.

Although formation of MgO clinker on the corroded test surface is observed, in both materials with graphite of 5 %(a) and 0 %(b) the clinker has poor continuity by intervening the pores. In the case of (a) large pore formed by corrosion with MgO-C reaction. On the other hand, in the case of (b), no large pore in the layer of MgO clinker is observed on the corroded test surface, and there is durable connecting layer was reserved. The formation of the pores due to MgO-C reaction in the specimen inside under the clinker layer was also significantly suppressed in the case of (b) compared with that of (a). Thus, it was apparent that the material without graphite showed higher corrosion resistance than those with graphite by preventing the clinker layer formed in the corroded surface from the penetration of Fe-oxide and the dispersion of Mg with MgO-C reaction, protecting the inside under the layer.

In the case of (c), which had the worst corrosion resistance test results, no large pore was observed on the corroded test surface like as the case of (b). On the other hand, the shape of the aggregate in the material E (c) was observed to be indistinct, unlike both the materials A (b) and D (a).

To investigate the difference in erosion between the materials A (b) and E (c), EPMA was used to analyze the microstructure. **Figure 5** shows the state of the hot surface of for both materials A (b) and E (c) after the Fe-oxide test. Focusing on the elemental distribution of iron, it was observed that in the A (b), the iron remained on the hot surface, while in the E (c), the iron infiltrated into the interior of the structure. Thus, the material A (a) was considered to have improved corrosion resistance where the infiltration of iron was more controlled than in the material E (b) .

3・4 Possible Improvement of Heat Dissipation

The heat conduction in the steady state was calculated on the assumption that four materials shown in the **Table 1** were applied respectively to the vessel wall (wear brick) in the lower vessel of the typical RH degasser. **Figure 6** shows the cross sectional view of the lower vessel of the RH degasser (a) and the part of area surrounded by the broken line was simplified to a model cylinder with (b), showing also layer composition of the vessel wall. 2500 mm height

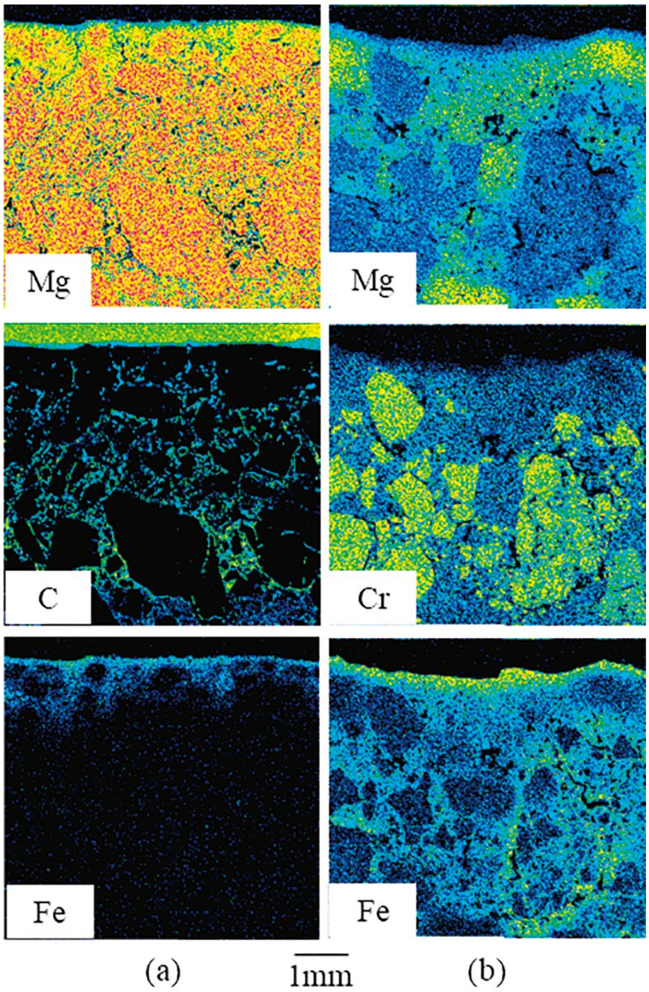

Fig. 5 EPMA analysis of the materials A (a) and the E (b) after the Fe-oxide test.

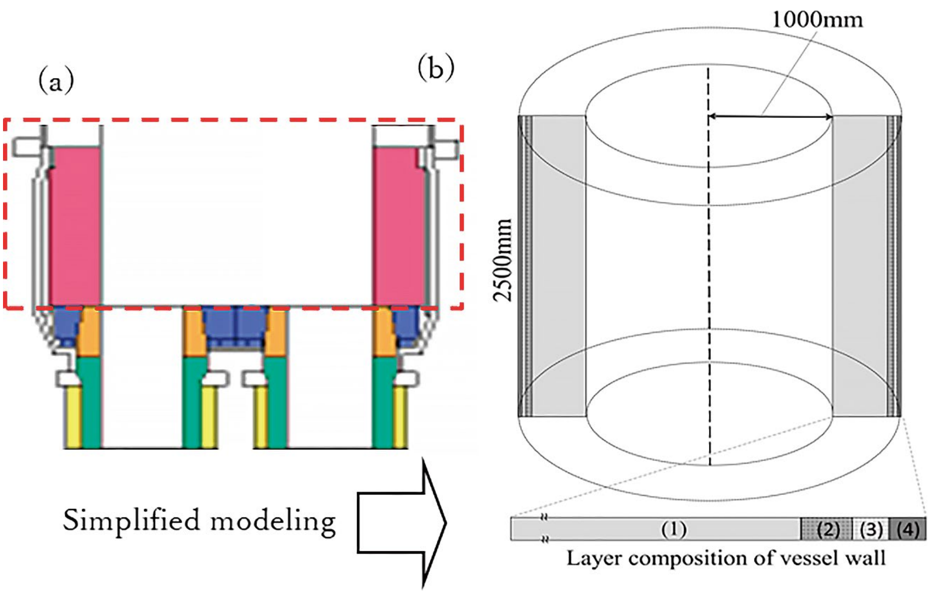

Fig. 6 Cross sectional view of the lower vessel of the typical RH* degasser(a) and the part of area surrounded by the broken line was simplified to a model cylinder(b) with wall composed by 4-layer materials shown in Table 3. (*RH: Ruhrstahl Heraeus degassing process)

Table 3 Condition for calculation of heat conduction in vessel wall

Layer composition of wall		Thickness /mm	Thermal conductivity, λ / $W \cdot m^{-1} \cdot K^{-1}$
(1)	Wear brick (inner)	450	4.0～9.5
(2)	Permanent brick	50	3.0
(3)	Insulating brick	30	0.1
(4)	Steel shell (outer most)	30	40.0

（=25 ℃）と接触して，外部へ熱を放射するものとし，この際，鉄皮の放射率εを0.85として計算した。**図7** に上記4材質を用いた場合の鉄皮温度及び熱流束の計算結果を示している。まず，図から明らかなように，黒鉛添加量が少ないほど，鉄皮温度は低く，黒鉛無添加の材質を用いることにより，黒鉛添加量5 mass%のれんがと比べて約16 ℃低くなることが判った。次に，熱流束も黒鉛添加量が少ないほど低減され，黒鉛無添加の場合，黒鉛添加量5 mass%のれんがと比べて約13 %低減することが明らかとなった。

上記の結果は，ウェアれんがの厚さが450 mmで一定として計算したが，実際の操業においては，ウェアれんがは溶損し，時間とともに薄化することを想定しなければならない。そこで，ウェアれんが4材質において，れんが厚さが450 mmから100

and 1000 mm distance from the center to the surface of the wear brick for the calculation. In addition, Table 3 shows thickness and thermal conductivity for 4-layer materials composing the wall as a calculation condition. The measured values shown in **Fig. 3 (a)** were used as the thermal conductivity of 4 materials in the **Table 3 (1)**.

Assuming steady heat conduction, heat release from the steel shell of the outermost layer in the vessel wall shown in **Fig. 6 (b)**, is estimated for the case that the inner and outer surface sides are contacting with 1600 ℃ molten steel and 25 ℃ air, respectively, and the emissivity of the steel shell as 0.85.

For 4 materials in the **Table 1**, the estimated both temperature of external steel shell and heat flux are shown in **Fig. 7** as a function of graphite amount in the materials. As shown in the **Fig. 7**, the temperature of steel shell lowered with the graphite content, and the temperature for the material without graphite was lower than that for the 5 % graphite content by about 16 ℃. Heat flux reduced also with

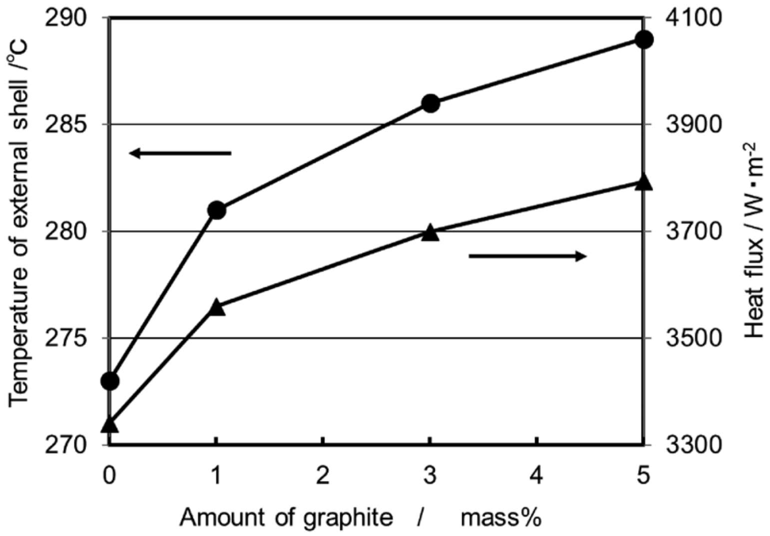

Fig. 7 Variations of temperature of exteranal steel shell, and heat flux with amount of graphite addition

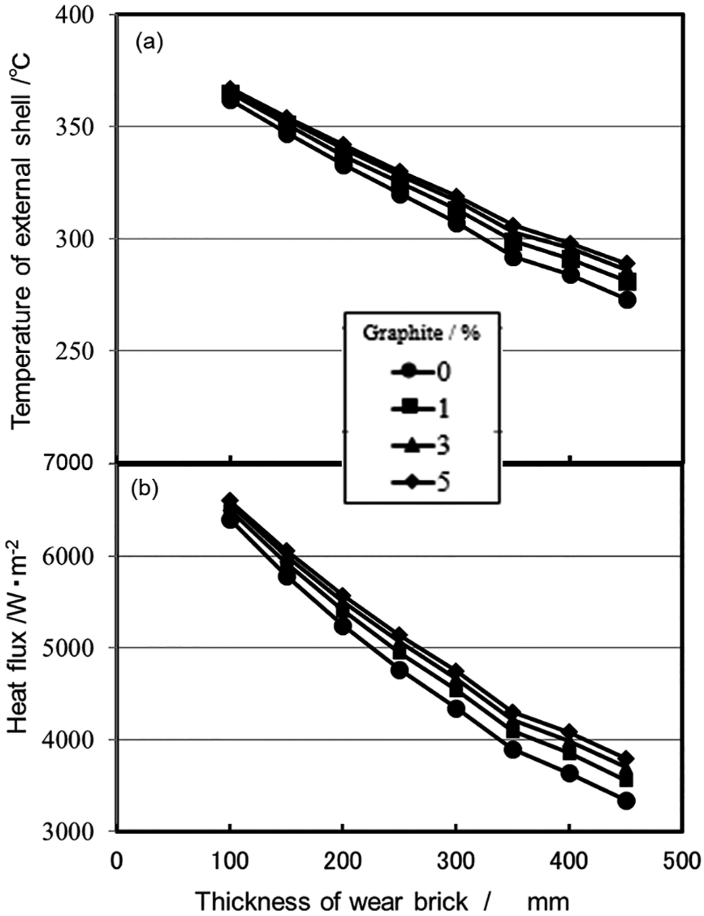

Fig. 8 Variations of temperature of exteranal steel shell (a), and heat flux (b) with thickness of wear brick for 4-kind of MgO-C system materials.

mm まで定速で溶損し薄くなると仮定した場合の鉄皮温度，熱流束の計算結果を**図 8（a）**および**（b）**にそれぞれ示している。各材質の場合とも，鉄皮温度，熱流束いずれもウェアれんがが薄くなるとともに上昇し，厚さ 100 mm の場合，鉄皮温度で約 30 %，熱流束で約 75 % の増大がみられた。

次に，4 材質をウェアれんがとして適用した RH 真空脱ガス装置下部槽の炉寿命 350 ch まで定速溶損するとし，1 回の処理時間を 30 分とした場合の稼働開始から終了までの累積放散熱量を式 (1) で計算し，計算結果を**図 9** に示している。

the graphite content as shown in **Fig. 7**, and the heat flux for the material without graphite decreased by about 13 % compared with that for the 5 % graphite content.

In the estimation performed so far, the heat release was calculated with the constant thickness of wear brick as 450 mm. In actual operation, however, the wear brick must be thinned with time due to erosion of molten steel. Thus, assuming that the brick is thinned to 100 mm at a constant rate, the temperature of both external shell and heat flux are calculated for the 4 materials with taking account of thinning of the wear brick during operation, as shown in **Fig. 8(a)** and **(b)**. As apparent in the figure, when the wear brick becomes 100 mm thickness, the temperature of external shell and heat flux increased from those for the original thickness of 450 mm by about 30 % and about 75 %, respectively.

Next, the accumulated heat radiation from the lower vessel of the RH degasser, Heat transfer amount Q was calculated using the equation (1) as

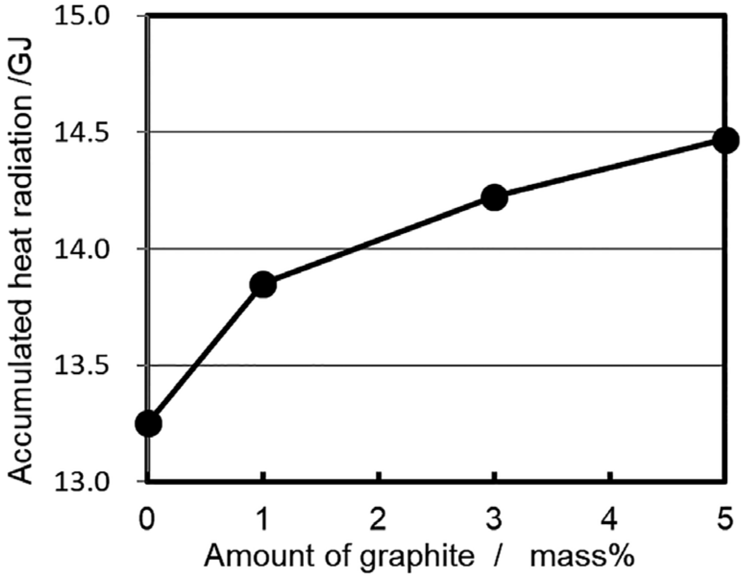

Fig. 9 Accumulated heat radiation of the lower vessel of RH degasser estimated for the cases of 4 MgO-C materials used as the wear brick of the furnace.

$$Q = h_c \cdot S \cdot \left(T_s - T_a\right) + \sigma \cdot \varepsilon \cdot S \cdot (T_s^4 - T_a^4) \quad (1)$$

hc：外部表面の対流熱伝達率 1.16 × 10^{-5} W/mm^2・K^{-1}

S ：伝熱面積

Ts：ウェアれんがの表面温度

Ta：外気温度

σ：ステファンボルツマン係数 5.67 × 10^{-14} W/mm^2・K^4

ε ：鉄皮の放射率 0.85

図 9 より，累積放散熱量は黒鉛添加量が少ないほど小さく，黒鉛を含まないれんがは黒鉛添加量 5 mass% のれんがより約 10 % 小さくなっていることから，熱ロスの抑制効果があることが明らかになった。

4 結言

黒鉛を含まない不焼成マグネシアれんがの特性は，黒鉛を含有するマグネシアカーボンれんがと比較して，かさ密度の低下，気孔率の上昇，弾性率の低下そして熱伝導率の低下が確認され，高熱 Fe-oxide に対して優れた耐食性を示すことが確認された。

shown in **Fig. 9**, when the 4 materials are applied to the wear brick of the vessel wall. As the assumption, total life of the lower vessel is considered as 350 ch with 30 min each.

$$Q = h_c \cdot S \cdot \left(T_s - T_a\right) + \sigma \cdot \varepsilon \cdot S \cdot (T_s^4 - T_a^4) \quad (1)$$

Where,

hc is convective heat transfer coefficient of external surface: 1.16×10^{-5} W/mm^2・K^{-1},

S is area of heat transfer,

Ts and *Ta* are temperatures of surface of the wear bricks and outside air, respectively,

σ is Stefan Boltzmann constant:5.67×10^{-14} W/mm^2・K^4 and

ε is emissivity of the steel shell: 0.85.

The accumulated heat radiation decreased with decreasing graphite content, and the heat radiation of the brick without containing the graphite was about 10 % lower than that with 5 % graphite content as shown in **Fig. 9**.

4 Summary

The characteristics of unburned graphite-free magnesia bricks were confirmed to be lower bulk density, higher porosity, and lower thermal conductivity in comparison with the bricks containing graphite. In addition to the expected suppression of the heat loss, due to low thermal conductivity, the

このことから，黒鉛を含有しない不焼成マグネシアれんがは，実使用における耐用性向上，鋼のカーボンピックアップの抑制の効果が期待でき，また熱ロスの抑制による CO_2 削減，そしてクロムを含まないことによる環境負荷低減に貢献できることが明らかである。

文　献

1) 中村義巳，菅野司，向所実，成田力也，土成昭弘，古川邦夫，北井恒雄：耐火物 , **49** [8] 478-479 (1997).
2) 清水公一，保木井利之，浅野敬輔，古澤正夫，三木隆：耐火物 , **53** [2] 84-85 (2001).
3) 阿南貴大，猿渡康允，田中雅人，吉富丈記：耐火物 , **67** [3] 166 (2015).
4) G. Ghosh, S. Haza, P. Chakraborty, S.Adak and A.K. Chattopadhyay : Proceedings of UNITECR 2009 (2009).
5) C. Pagliosa, A. Campos, B. Borges, V. Madalena and V.C. Pandolfelli : Proceedings of UNITECR 2019 (2019).
6) B. Borges, C. Pagliosa, M. Borges, A. Campos, V. Madalena, and V.C. Pandolfelli : Proceedings of UNITECR 2022 (2022).
7) M. Tanaka, H. Kamio, J. Yoshitomi, T. Kayama, S. Hanagiri and K. Goto : Proceedings of UNITECR 2011 (2011).
8) 淵本博之，平尾啓典，大崎博右，保木井利之，清水勇：耐火物, **52** [3] 136-137 (2000).
9) 松堂人士，中谷友彦，津田智裕，小出邦博，福田知美：耐火物, **66** [3] 145 (2014).

本論文は以下の報文に加筆・再構成して転載したものである。
Yuya Tomita et al.: Proceedings of UNITECR2023 (2023) pp.364-367.
冨田他：第 14 回環境と耐火物研究会報告集，耐火物技術協会 (2015) pp.15-23.

unburned graphite-free magnesia brick showed higher corrosion resistance against Fe-oxide at high temperature than the MgO-C (graphite) bricks. Thus, in the practical use of the unburned graphite-free magnesia brick, the steel making process is expected to be improved by increasing durability of refractories for the secondary refining, by decreasing the environmental loading through both CO_2 reduction and chromium eliminations from the refractories, and by minimizing the opportunity of the steel to pick-up carbon from the refractories.

References

1) Y. Nakamori, T. Kanno, M. Mukaijo, R. Narita, A. Tsuchinari, K. Furukawa and T. Kitai. : TAIKABUTSU, **49** [8] 478-479 (1997).
2) K. Shimizu, T. Hokii, K. Asano, M. Furusawa and T. Miki. : TAIKABUTSU, **53** [2] 84-85 (2001).
3) T. Anan, Y. Saruwatari, M. Tanaka and J. Yoshitomi : TAIKABUTSU, **67** [3] 166 (2015).
4) G. Ghosh, S. Haza, P. Chakraborty, Dr. S.Adak and Dr. A.K. Chattopadhyay : Proceedings of UNITECR 2009 (2009) .
5) C. Pagliosa, A. Campos, B. Borges, V. Madalena and V.C. Pandolfelli : Proceedings of UNITECR 2019 (2019) .
6) B. Borges, C. Pagliosa, M. Borges, A. Campos, V. Madalena, and V.C. Pandolfelli : Proceedings of UNITECR 2022 (2022) .
7) M. Tanaka, H. Kamio, J. Yoshitomi, T. Kayama, S. Hanagiri and K. Goto : Proceedings of UNITECR 2011 (2011).
8) H. Fuchimoto, H. Hirao, H. Osaki, T. Hokii and I. Shimizu. : TAIKABUTSU, **52** [3] 136-137 (2000).
9) H. Matsudo, T. Nakatani, T. Tsuda, K. Koide and T. Soeda : TAIKABUTSU, **66** [3] 145 (2014).

This paper is reprinted with some additions and erconstructions to the following papers:
Yuya Tomita et al.: Proceedings of UNITECR2023 (2023) pp.364-367.
Yuya Tomita et al.: Proceedings of 14th Symposiun on Environment and Refractories, Technical Association of Refractories, Japan (2015) pp.15-23.